What can we learn about hadronic intermittency from finite fractal sets?

T. Hakioğlu
Physics Department, University of Arizona, Tucson, Arizona 85721
(Received 18 September 1991)

The formalism recently introduced in hadronic intermittency is used to understand the dynamics of one-dimensional fractal sets. We examine the translation invariance, factorial and cumulant moments, and the fractal dimensions of the phase space as the nonlinearity of the sets is changed in a broad range from intermittent to chaotic. We show that the dynamical content of the sets is strongly interwoven with the magnitude of the fractal dimensions of the phase-space correlations. We simulate events by properly transforming the logistic map so that relevant density histograms of hadronic particle distributions are qualitatively produced. We use this as a toy model to understand the rapidity phase-space behavior of these distributions. By studying the fractal dimensions of these models we show that the hadronic data show very weak intermittency in the rapidity phase space.

PACS number(s): 13.85.Hd, 05.45.+b, 12.40.Ee, 24.60.Lz

I. INTRODUCTION

Perhaps the most striking experimental observation of the last 30 years in high-energy physics is the fact that the hadronization process has a large contribution from fractal dynamics [1]. The question of coherence vs chaos in high-energy collisions has been around since the 1960s, and it was raised by the Goldhaber-Goldhaber-Lee-Pais experiment [2]. Full analogy with the already well-developed quantum optics (QO) was made by measuring the "pion-bunching" effect, an analogue of the Hanbury Brown–Twiss (HBT) photon-bunching effect [3] in QO. In the hadronic HBT [4] effect, by measuring the hadronic analogue of the quantum optical intensity correlation function, one observes a large contribution from chaotic dynamics. This was the main drive for the studies on distributions relevant to QO, such as Poisson or negative binomial distributions (NBD), to fit the hadronic probability distributions [5] which are, respectively, coherent and chaotic limits of the generalized Bose-Einstein distribution. Successful NBD fits [1] for non-nucleus-nucleus collisions confirm the presence of a large chaotic contribution.

Recently attention in high-energy physics has been focused on the short-range analysis of hadronic rapidity correlations by the use of factorial moments. In the factorial moment technique [6], the full rapidity window $2Y$ is divided into M identical bins of width $\delta y = 2Y/M$. For ideal resolution, the single-particle density distribution $\hat{\rho}_1(y,\mathbf{s})$ is

$$\hat{\rho}_1(y,\mathbf{s}) = \sum_i \delta(y - s_i) , \tag{1.1}$$

where s_i indicates the rapidity location of particle i. The notation $\mathbf{s} = \{s_i, i=1,\ldots,N\}$ denotes a particular member (event) of an ensemble (set of events) $\{\mathbf{s}\}$. In general the p-particle correlation density is

$$\hat{\rho}_p(y_1,y_2,\ldots,y_p;\mathbf{s}) = \prod_{a=1}^{P}{}' \sum_{i=1}^{N} \delta(y_a - s_i) , \tag{1.2}$$

where the prime indicates that $y_1 \neq y_2 \neq \cdots \neq y_p$. The event average $\langle \hat{\rho}_p(y_1,y_2,\ldots,y_p) \rangle$ gives the correlation function

$$\rho_p(\{y_p\}) = \langle \hat{\rho}_p(y_1,y_2,\ldots,y_p) \rangle = \int ds\, Q(\mathbf{s}) \hat{\rho}_p(y_1,\ldots,y_p,\mathbf{s}) , \tag{1.3}$$

where $Q(\mathbf{s})$ performs the average over the ensemble [7].

The knowledge of (1.1)–(1.3) is basically all that is needed to build a hierarchy of p-point correlation functions $\rho_p(y_1,\ldots,y_p)$. Then the factorial moments F_p are given in terms of $\rho_p(y_1,\ldots,y_p)$'s integrated in the proper domains $\Omega_i^{(p)}$ of the p-dimensional rapidity space [8],

$$F_p(\delta y) = \frac{1}{M} \sum_{i=1}^{M} \frac{1}{(\delta y)^p} \int_{\Omega_i^{(p)}} dy_1\, dy_2 \cdots dy_p \times \frac{\rho_p^{(i)}(y_1,\ldots,y_p)}{(\rho_1^{(i)})^p} , \tag{1.4}$$

where $\Omega_i^{(p)}$ is a hypertube of volume $2Y(\delta y)^{p-1}$ centered around $\mathbf{y} = \{y_i,\ldots,y_p\}$. The relation (1.4) counts the event-averaged number of particles in the volume $\Omega_i^{(p)}$ and then averages over M hypercubes. In other words, the factorial moments are [6],

$$F_p(\delta y) = \frac{1}{M} \sum_{i=1}^{M} \frac{\langle n_i(n_i-1)\cdots(n_i-p+1) \rangle}{\langle n_i \rangle^p} , \tag{1.5}$$

where $\langle n_i \rangle = \rho_1^{(i)} \delta y$.

By converting the rectangular coordinates into the center-of-mass (c.m.) ones [e.g., $\eta = (1/p)\sum_{i=1}^{p} y_i, \xi_{ij} = y_i - y_j$], the physical meaning of the bin averaging becomes clearer. The integration over the c.m. normalized by the rapidity window $2Y$, becomes to a good approximation [9]—in the experimentally relevant bin sizes this approximation is good up to 80–95 %—the average over M bins:

$$\frac{1}{M} \sum_{i=1}^{M} (\text{bins}) \to \frac{1}{2Y} \int_{-Y}^{Y} d\eta . \tag{1.6}$$

This area-preserving transformation from the rectangular to c.m. variables is particularly suited to the common situation in hadronic distributions where correlation functions are short range [8] (correlation length is smaller than $2Y$, for instance, even in the worst example of translation invariance for the NA22 data $\xi \simeq 1.35$ and $Y \simeq 2.5$) and approximately translationally invariant in the central rapidity domain.

In terms of the new variables,

$$F_p(Y,\delta y)=\frac{1}{2Y}\int_{-Y}^{Y} d\eta \int_{-\delta y/2}^{\delta y/2}\{d\xi_{ij}\}\frac{\rho_p(\{\xi_{ij}\},\eta)}{\langle n\rangle^p} , \quad (1.7)$$

where $\langle n\rangle = \delta y \rho_1$ and there are $(p-1)$ relative coordinates $\xi_{ij}, i=1,\ldots,p$. For translationally invariant rapidity distributions the η dependence in Eq. (1.7) drops out, and one obtains a more traditional definition, Eq. (1.5), of the factorial moments. Both definitions, Eqs. (1.5) and (1.7), have pros and cons. For ideal resolution given by Eq. (1.1), the latter reduces to conventional Grassberger-Proccacia (GP) moments [10] which, although manifestly translation invariant and intuitive, are much slower and cumbersome for numerical calculations than the simpler equation (1.5) [11,12]. On the other hand, Eq. (1.7) has been developed for fitting the short-range correlations, and it also is the only candidate to derive the explicit formulas of the linked-pair approximation [8]. We also note that Eq. (1.7) is superbly advantageous for testing translation invariance.

Previously, experimental [13] and theoretical [6,7,14] works on multihadron production at high energies have explored the dependence of bin-averaged factorial moments, (1.5) and (1.7), on the size δy of the rapidity bin. Below a certain range of δy, the moments approximate a power law which has become known as *intermittency* in high-energy physics. Apparently, in this particular case, a familiar thing happens, that is, the one-to-one correspondence between experiment and theory seems to break down, and a variety of theoretical models (from the self-similar cascade α model [6] to exponential and short-range correlation [7,8]) can be well fitted to the experimental data within the errors. Traditionally, intermittency refers to a stochastic process in which periods of fluctuating dynamics are interspersed with quiescence. The power law is typical of fractal geometry, of which traditional intermittency is a special case. Chaotic and self-similar cascading models are examples of this behavior.

In this work we investigate the idea of simulating the hadronic data by using one-dimensional fractal sets. The relevant question is: Can a given rapidity histogram be realized as a finite sample of a strange attractor (fractal set) embedded in the multihadron S matrix? This question leads us to start from the opposite end: If we generate data by choosing a qualitatively suitable fractal set, can we reproduce physically relevant histograms and correlation functions? In Sec. II we describe how to generate such rapidity histograms deterministically from one-dimensional finite fractal sets. We then study the factorial moments and cumulants in different dynamical regimes of these sets as the strength of the intermittency vs deterministic chaos is changed by a nonlinearity parameter. We focus on the question of translation invariance under these dynamically different conditions. In Sec. III, we describe a particular model and analyze the translation invariance (TI) and the phase-space dimensionality by the use of factorial moments. We give examples from various hadronic data fits to qualitatively compare the model and the data. We use the word rapidity in a generic fashion for the phase-space variable throughout the work.

II. RAPIDITY HISTOGRAMS FROM FRACTAL SETS

It was shown in Refs. [12,15] that the one-dimensional triangular map in the interval $-0.5 \le x \le 0.5$,

$$x_{n+1}=f(x_n)=\begin{cases}2\lambda(0.5+x_n), & x\le 0 ,\\ 2\lambda(0.5-x_n), & x>0 ,\end{cases} \quad (2.1)$$

with $\lambda \ge 0.5$, is fully chaotic and represents a deterministic Gaussian white noise. Namely, the autocorrelation is

$$R(m)=\lim_{N\to\infty}\frac{1}{N}\sum_{i=1}^{N} x_{i+m}x_i \propto \delta_{m,0} , \quad (2.2)$$

and the mean-square distance $R(0)\propto N$, with $\langle x\rangle = 0$ simulating a Brownian motion. In the two-dimensional phase space x_{n+1} vs x_n iterates fill the triangular area given by (2.1) uniformly. As a result of this the invariant density of points is unity:

$$\rho_f(x)=\sum_{n=0}^{\infty}\delta(x-f^{(n)}(x_0))=1 , \quad (2.3)$$

where $f^{(n)}(x_0)=f[f[\cdots[f(x_0)]\cdots]]$ is the functional iteration of order n starting from x_0. One can modify the map (2.1) so that the invariant density (2.3) is convex and qualitatively fits to a hadronic density histogram produced by a finite number of particles. Applying the transformation

$$x_n=\sinh(y_n/r) , \quad (2.4)$$

we obtain the modified triangular map

$$y_{n+1}=g(y_n)=\begin{cases}(1/r)\sinh\{2\lambda[0.5+\operatorname{arcsinh}(ry_n)]\}, & y\le 0 ,\\ (1/r)\sinh\{2\lambda[0.5-\operatorname{arcsinh}(ry_n)]\}, & y>0 .\end{cases} \quad (2.5)$$

The invariant density of (2.5) then becomes

$$\rho_f(y)=\frac{r}{\sqrt{1+y^2}} . \quad (2.6)$$

The histogram corresponding to (2.6) is shown in Fig. 1.

Obviously such a one-to-one mapping as given by (2.4) does not alter the underlying dynamics. As a result of this the modified triangular map (2.5) is also Brownian.

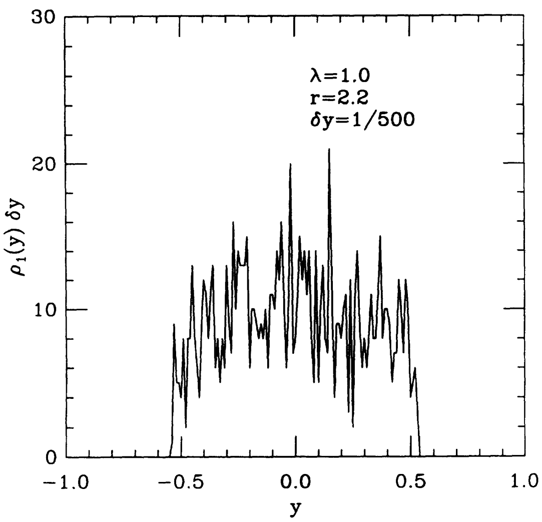

FIG. 1. Histogram of an event created by the transformed triangular map (2.5).

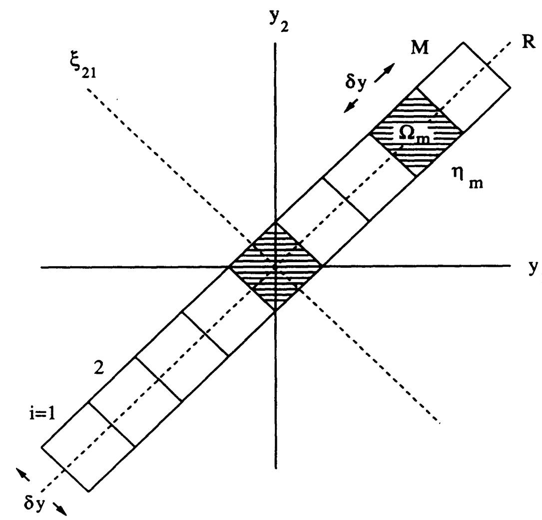

FIG. 3. Strip-domain approximation and testing of the translation invariance.

This time we verify this by numerically computing the factorial moments of Eq. (2.5) using Eq. (1.5). The structureless moments with decreasing δy in Fig. 2 indicate that the correlations are as short as they can be [i.e., $R(m)\propto\delta_{m,0}$], as expected from a Gaussian distribution. We have generated the $F_p(\delta y)$ using $N=200$ particles/event averaged over 1000 events. Different events were generated by randomly shifting the initial setting $y_0=(1/r)\mathrm{arcsinh}x_0$ using a uniform distribution.

An essential point in Eq. (1.5) is the bin average. Averaging over the bins with equal weight is only justified when translation invariance (TI) is a good approximation. To justify TI one would like to know how smooth the density of points for a fixed value of c.m. is. For this purpose we introduce $\Delta(\eta,\delta y)$:

$$\Delta(\eta,\delta y)=\int_{-\delta y/2}^{\delta y/2}d\xi\int_{\eta-\delta y/2}^{\eta+\delta y/2}dR\ \langle\hat{\rho}_2(y_1,y_2)\rangle\ , \qquad (2.7)$$

which is nothing but the two-particle factorial moment defined in one of the M bins centered at $\eta=(y_1+y_2)/2, y_1-y_2=0$, as shown in Fig. 3.

Obviously, for translationally invariant problems, $\langle\hat{\rho}_2(y_1,y_2)\rangle$ does not depend on R; thus $\Delta(\eta,\delta y)$ is independent of η. Another version of (2.7) is in terms of c.m. coordinates:

$$\Delta(\eta,\delta y)=\int_{-\delta y/2}^{\delta y/2}d\xi\int_{\eta-\delta y/2}^{\eta+\delta y/2}dR\ \langle\rho_1(R-\xi/2)\rho_1(R+\xi/2)\rangle\ . \qquad (2.8)$$

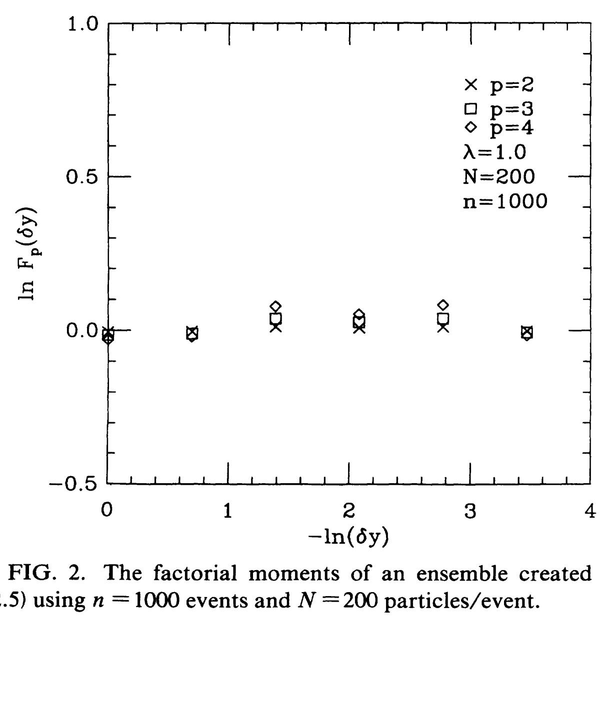

FIG. 2. The factorial moments of an ensemble created by (2.5) using $n=1000$ events and $N=200$ particles/event.

For instance, the manifestly smooth rapidity density

$$\rho_1(y)=\frac{1}{2Y}\theta(Y-|y|)\ \text{ gives }\ \Delta(\eta,\delta y)=\left[\frac{\delta y}{2Y}\right]^2 . \qquad (2.9)$$

Applying this technique to the modified triangular map, Eqs. (2.5) and (2.6), yields a measure for the quality of the translation invariance as parametrized by the rapidity bin size. Figure 4(a) represents $\Delta(\eta,\delta y)$ normalized to the central bin $\eta=0$. Translation invariance is valid up to 20% with its maximum violation close to the edges of the rapidity window $2Y$ as $\eta\to Y$. The relative magnitude of δy also does not affect TI more than 0.5%. In Fig. 4(b), $\Delta(0,\delta y)$ is shown to scale approximately by

$$\Delta(0,\delta y)\propto\delta y^{1.962}\ . \qquad (2.10)$$

This indicates that the transformation (2.4) does not change the TI of the original map (2.1). In short we can safely assume the modified triangular map is a translationally invariant system.

III. GENERATING THE INTERMITTENCY BY FRACTAL SETS

Intermittency is a transitory phenomenon between two well-defined phases of a nonlinear system that are characterized by regular (periodic, laminar, etc.) and chaotic (asperiodic, turbulent, etc.) fluctuations. Whether the system is a real one or a numerical model, the time record of an observable is such that the regular behavior seems to be randomly and abruptly disturbed by time bursts. The burst separating two time sectors is of finite duration. The average burst frequency is random and larger than the characteristic frequency of the regular fluctuations [16].

Let us describe a dynamical time evolution $y(t)$ at a Poincaré sector of the entire phase space by the time series

$$y_{n+1}=F(y_n,a) , \tag{3.1}$$

where a is the nonlinearity control parameter. Generic features of intermittency as described above can be reproduced by a time series similar to Eq. (3.1) at values of a very close to the value a_c at a tangential limit cycle [12]. This general description, i.e., tangent bifurcations, can be seen in the Lorentz model [17,18] or in the logistic map [19].

A. The logistic map

Having this "quasi-analytical" description of intermittency, we here, by the method described in Sec. I, analyze the behavior of the factorial moments and cumulants in different dynamical regimes of the "data" generated by the logistic map

$$x_{n+1}=F(x_n,a)=ax_n(1-x_n), \quad 0\le x\le 1, \; 0\le a\le 4 . \tag{3.2}$$

At the parameter value $a=4$, Eq. (3.2) is fully chaotic. The invariant density $\rho(x)$ can be analytically found to be

$$\rho(x)=\frac{1}{\pi\sqrt{x(1-x)}} . \tag{3.3}$$

By applying the smooth invertible transformation

$$x_n=\frac{e^{2y_n}}{1+e^{2y_n}} , \tag{3.4}$$

we obtain the transformed logistic map (TLM)

$$y_{n+1}=\frac{1}{2}\ln\left|\frac{ax_n(1-x_n)}{1-ax_n(1-x_n)}\right|, \quad -\infty<y<\infty , \tag{3.5}$$

which also describes a similar dynamical system, but with a different invariant density described as

$$\rho(y)=\frac{2}{\pi}\frac{e^{2y}}{1+e^{2y}} . \tag{3.6}$$

The corresponding histogram of Eq. (3.6) integrated in the range $-3\le y\le 3$ (i.e., $2Y=6$) with a finite small bin size $\delta y=\frac{1}{150}$ is given in Fig. 5. In the interval $3.83<a\le 4$

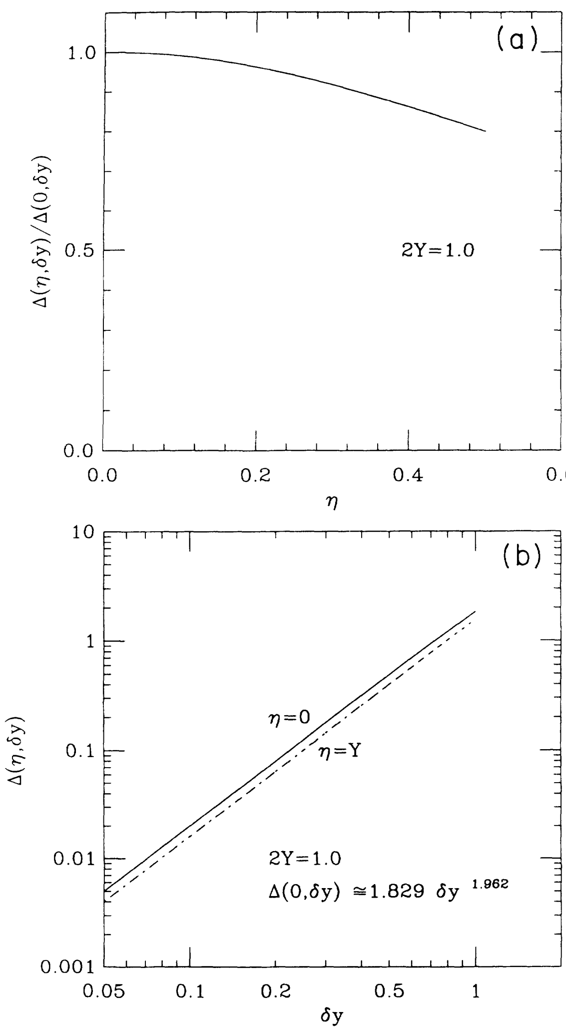

FIG. 4. Translational invariance in the transformed triangular map.

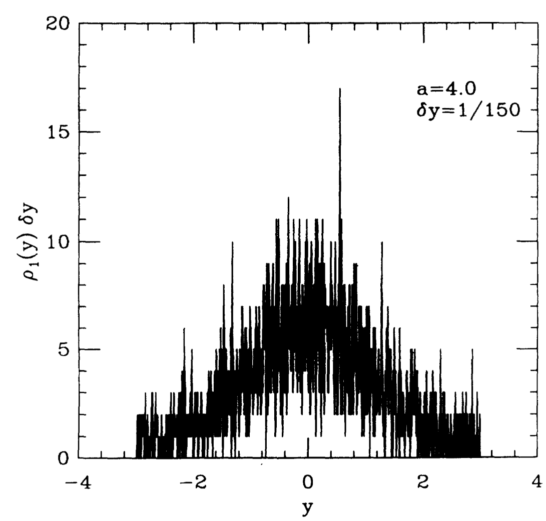

FIG. 5. Histogram of an event created by the fully chaotic ($a=4$) TLM.

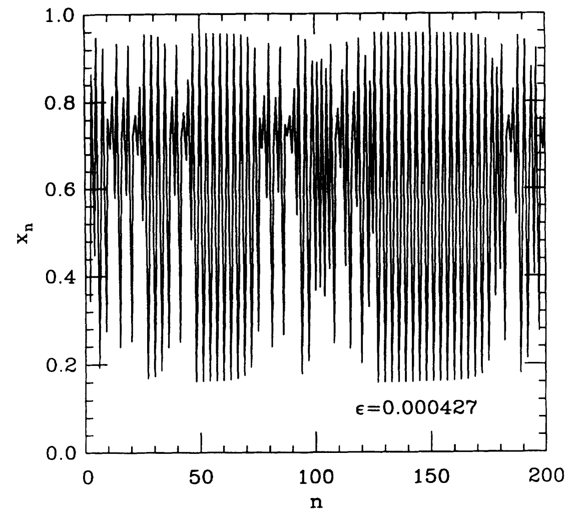

FIG. 6. Time evolution of iterates in the intermittent TLM.

the map (3.2) remains chaotic (i.e., Lyapunov exponent $\lambda \geq 0$). Particularly for $a_c = 1+\sqrt{8}$, a three-period cycle is observed through tangent bifurcations [17–19]. These odd-period cycles appear in between chaotic bands down to $a \simeq 3.57$, below which stable even-period cycles are observed. Intermittency is observed at values just below where the odd-period cycles appear; $a = a_c - \epsilon$ where $0 < \epsilon \ll 1$. Figure 6 describes a typical intermittent time evolution of the iterations for $a_c - a = \epsilon = 0.000\,426 \ll a_c$. As $a \to a_c$, e.g., $\epsilon \to 0$, the average time interval between random bursts grow as $\epsilon^{-1/2}$, yielding a regular signal fluctuating between three fixed points $x_1 = 0.160$, $x_2 = 0.514$, $x_3 = 0.956$ [19].

B. The question of translation invariance

By using the measure $\Delta(\eta, \delta y)$, we can examine the translation invariance of the fully chaotic logistic map. The invariant density, Eq. (3.3), is divergent at the edges [0,1] of the distribution. This results in the convolution integral (2.8) having a singularity at $\eta = 1$, as shown in Fig. 7(a). The strength of the singularity increases proportionally to the inverse bin size, a fact that cannot be seen in TI cases. Figure 7(b) represents the parametric dependence of $\Delta(\eta, \delta y)$ on the c.m. as a function of δy. This function is quite entangled in the variables η and δy so that factorization such as in the simple case (2.9) does not seem possible.

Next we examine the fully chaotic TLM. This time using $\rho_1(y)$ given by (3.6), the numerical computation of $\Delta(\eta, \delta y)$ suggests a quite different behavior of TI as compared to its untransformed counterpart, Eq. (3.2). The effect of the transformation is already seen by the comparison of the divergent equation (3.3) and the much smoother transformed version (3.6). Figure 8(a) shows independence of the ratio $\Delta(\eta, \delta y)/\Delta(0, \delta y)$ from δy obtained for a large range $\delta y / 2Y = 0.1-0.01$. This suggests a factorization of the variables as

$$\Delta(\eta, \delta y) = \Delta(0, \delta y)(1 + C\eta^{\alpha}) , \tag{3.7}$$

where we found $\alpha = 0.344$ and $C \simeq 1.17$ (e.g., constant). From Fig. 8(b) we find

$$\Delta(0, \delta y) \simeq 0.2\delta y^{2.051} . \tag{3.8}$$

The TI of the TLM is badly broken, up to 300% towards the edge of the rapidity distribution. Towards the central region the full TI is recovered as shown in Fig. 8(b). By comparison, we deduce that a simple one-to-one nonlinear transformation changes the strong uniformity of (3.3) into a controllable violation of TI.

For invariant densities given functionally as (2.6), (3.3), and (3.6) the application of formula (2.8) is a matter of integration. Below the fully chaotic regime we have only numerically accessible histograms of finite samples, not invariant densities. For such discrete problems the interpretation of (2.8) is quite simple. Characterizing a particular bin by Ω_m and η_m, the integration in (2.8) becomes

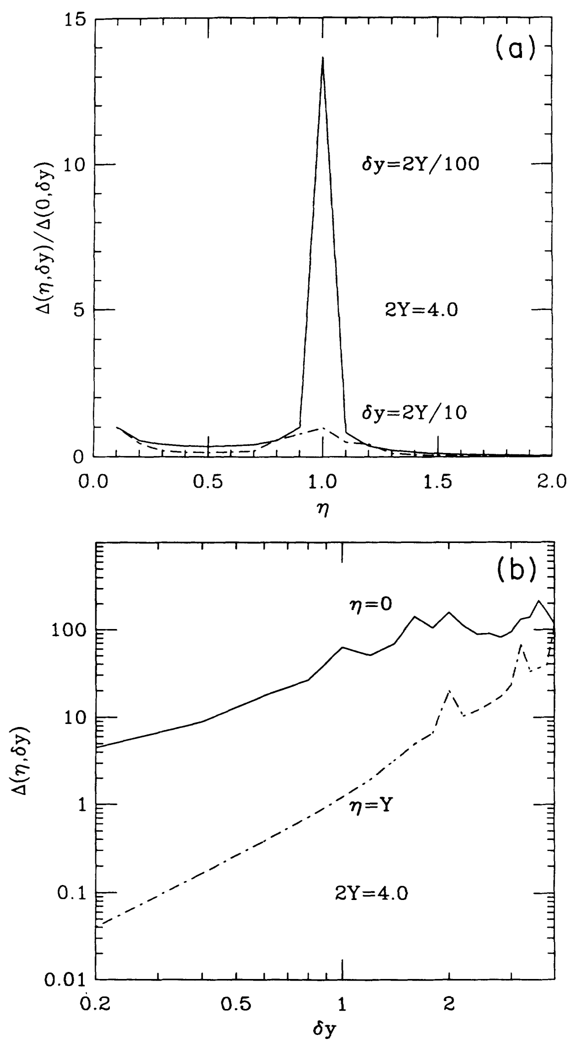

FIG. 7. (a) c.m. dependence and translation invariance of the fully chaotic logistic map. (b) Bin-size dependence and translation invariance of the fully chaotic logistic map.

$$\Delta(\eta_m,\delta_y)=\int_{-\delta y/2}^{\delta y/2} d\xi \int_{\eta_m-\delta y/2}^{\eta_m+\delta y/2} dR\ \langle \rho_1(R-\xi/2)\rho_1(R+\xi/2)\rangle$$
$$=\langle n(n-1)\rangle_{\Omega_m}\ , \tag{3.9}$$

which is just the factorial moment defined for the phase-space volume Ω_m centered at η_m, as described by the shaded squares in Fig. 3. Equation (3.9) can be computed for a finite set easily. Specifically, we give results for the TLM at the onset of intermittency in Fig. 9. Here again, at smaller bin sizes, the nonuniformity is indefinitely enhanced; the same behavior that was observed for the untransformed logistic map as well. This effect seems to be a consequence of the divergences in the invariant density (histogram).

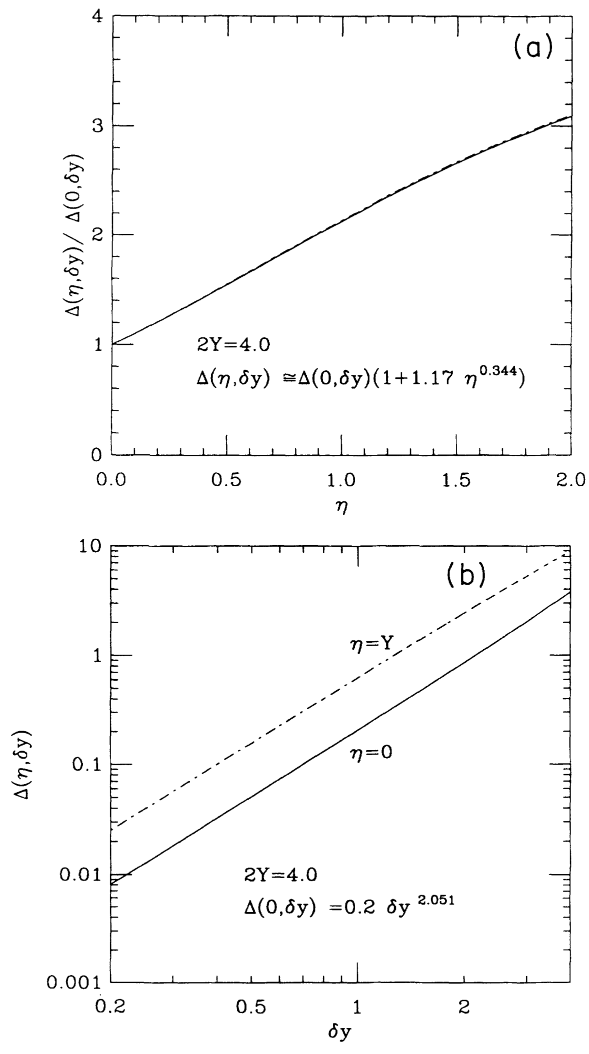

FIG. 8. (a) c.m. dependence and translation invariance of the fully chaotic TLM. The dashed and the solid lines correspond to $\delta y/2Y=0.01$ and $\delta y/2Y=0.1$, respectively. (b) Bin-size dependence and translation invariance of the fully chaotic TLM.

C. Factorial moments and cumulants

1. Factorial moments

Except for generating a physically interesting rapidity histogram at the chaotic threshold, the underlying dynamics of Eq. (3.5) is not different from the original logistic map. The values of the critical parameter a_c between regular and irregular regimes are given by the same set of values in both. This is a result of the smoothness of the transformation (3.4), by which no dynamics is added. At the onset of intermittency, where $a=a_c-\epsilon$ for $a_c=1+\sqrt{8}$ and $0<\epsilon\ll 1$, we have observed a perfect scaling for the moments of the TLM as functions of δy, as shown in Fig. 10. The scaling law in this figure is violated for $\delta y>1$ due to the finite interval in which the map is defined. The measured slopes correspond to the scaling indices ν_p of the moments F_p,

$$\ln F_p(\delta y)=A_p-\nu_p \ln\delta y\ . \tag{3.10}$$

The curves indicate that $A_p\simeq 0$ and

$$\nu_2\simeq 0.9625,\quad \nu_3\simeq 1.9531,\quad \nu_4\simeq 2.9501\ . \tag{3.11}$$

The ratio ν_p/ν_2 can be well fitted to that of a monofractal

$$\nu_p/\nu_2=p-1 \tag{3.12}$$

by

$$\nu_3/\nu_2\simeq 2.0293 \quad\text{and}\quad \nu_4/\nu_2\simeq 3.0650\ . \tag{3.13}$$

The fact that the ν_p's in (3.11) are almost integral num-

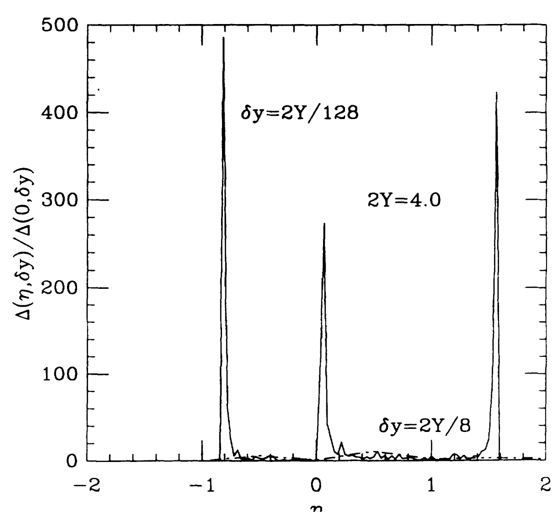

FIG. 9. c.m. dependence and translation invariance of the intermittent TLM.

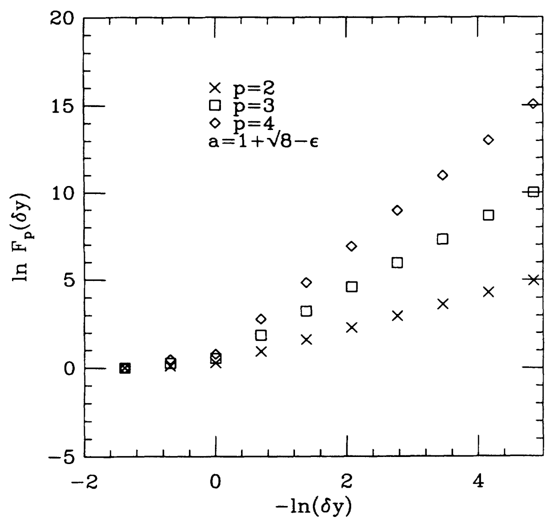

FIG. 10. Factorial moments of the intermittent TLM.

bers can be explained in terms of the fractal dimensionality of rapidity-bin hypertubes $\Omega^{(p)}=2Y(\delta y)^{p-1}$ by the use of Grassberger-Proccacia (GP) moments [10,11]. Integrating Eq. (1.7) in the center-of-mass strip domain, in the case of ideal resolution such as Eq. (1.1) with s_i's generated by a map such as (3.5), yields the factorial moments in terms of GP ones:

$$F_p(\delta y)=\frac{1}{M}\frac{\Gamma_p(\delta y)}{\langle n\rangle^p}\ , \qquad (3.14)$$

where

$$\Gamma_p(\delta y)=N^p I_p(\delta y)\ , \qquad (3.15)$$

where $N=\langle n\rangle M=200$ is the total number of particles in one event and $I_p(\delta y)$ is the generalized pth-order pair-correlation function [12,15]

$$I_p(\delta y)=\frac{1}{N^p}\sum_{\substack{i,j,\ldots,s,p=1\\ i\neq j\neq l\neq\cdots s\neq p}}^{N}\theta_1(\delta y-|\xi_{ij}|)\theta_2(\delta y-|\xi_{jl}|)\times\cdots\theta_{p-1}(\delta y-|\xi_{sp}|)\ . \qquad (3.16)$$

$\Gamma_p(\delta y)$ is the factorial moment given by

$$\Gamma_p(\delta y)=\int_{-\delta y/2}^{\delta y/2}\{d\xi_{ij}\}\rho_p(\{\xi_{ij}\})=\langle n(n-1)\cdots(n-p+1)\rangle\ , \qquad (3.17)$$

where we customarily use translation invariance,

$$\rho_p(\{\xi_{ij}\},\eta)=\rho_p(\{\xi_{ij}\})\Longrightarrow\langle n_i\rangle=\langle n\rangle=N/M\ .$$

Physically $I_p(\delta y)$ counts the number of particles in a p-dimensional hypertube $\Omega^{(p)}=2Y(\delta y)^{p-1}$ [the cross section corresponds to a $(p-1)$-dimensional square, and the tube axis is integrated along the c.m. coordinate] obtained by the direct product of p identical rapidity distributions. Hence, as $\delta y\to 0$, (3.16) is proportional to the fractal dimensionality γ_p of $\Omega^{(p)}$. Therefore,

$$I_p(\delta y)|_{\delta y\to 0}\sim(\delta y)^{\gamma_p}\ . \qquad (3.18)$$

Then we obtain, using (3.12) and (3.15),

$$F_p(\delta y)=M^{p-1}I_p(\delta y)|_{\delta y\to 0}\sim(2Y)^{p-1}\left[\frac{1}{\delta y}\right]^{p-1-\gamma_p}\ . \qquad (3.19)$$

Thus $\nu_p=p-1-\gamma_p$. There are two extreme limits on the scaling characteristics of Eq. (3.19). For a uniform rapidity distribution [i.e., $\rho(y)=\text{const}\neq 0$] the direct product of p uncorrelated spaces results in $\gamma_p=(p-1)$, and no scaling is present in $F_p(\delta y), \nu_p=0$. Contrary to the strong uniformity in the rapidity distribution, in the case of strong intermittency, particles are generated in the phase space with a strong nonuniformity. Such cases include random spikes and voids in the histograms. In such circumstances a few spikes determine the whole number average, and the fractal dimensionality of the rapidity distribution is approximately that of a point (e.g., $0<\gamma_2\ll 1$). This specific example of strong intermittency is seen in the TLM at $a=a_c-\epsilon$ as $\epsilon\to 0^+$ as three spikes in the rapidity distribution resulting from a stable three-cycle period. Since $0<\gamma_1\ll 1$, this results in $0<\gamma_p\ll 1$ and $\nu_p\le p-1$ as observed in (3.11). The small marginal difference from the upper integral value is the fractal dimension in the GP moments, which are $\gamma_2\simeq 0.0375$, $\gamma_3\simeq 0.0469$, $\gamma_4\simeq 0.0499$ obtained for $\epsilon=0.00427$. From the ratios of γ_p's we notice that the direct produce space is far from being uncorrelated (e.g., dimensions are coupled).

Next we consider the factorial moments in the chaotic regime. As the full chaoticity at $a=4$ is approached, uniformity is gradually recovered, and one expects the factorial moments to gradually level off. For instance, at $a=3.9$ we numerically found

$$\nu_2\simeq 0.0753,\quad \nu_3\simeq 0.2218,\quad \nu_4\simeq 0.4535\ , \qquad (3.20)$$

and the ratio ν_p/ν_2 is well fitted to that of a log-normal distribution [6] (i.e., in multiplicative Gaussian random variables)

$$\frac{\nu_p}{\nu_2}=\frac{1}{2}p(p-1) \qquad (3.21)$$

by $\nu_3/\nu_2\simeq 2.945$ and $\nu_4/\nu_2\simeq 6.022$. The fractal dimensionality of the direct product space γ_p is found to be $\gamma_2\simeq 0.9247$, $\gamma_3\simeq 1.9982$, and $\gamma_4\simeq 2.5465$. In this case, the ratios γ_p/γ_{p-1} are

$$\gamma_3/\gamma_2\simeq 2.1619,\quad \gamma_4/\gamma_3\simeq 1.2743\ , \qquad (3.22)$$

and, as compared to the intermittent case, are much closer to those expected from the manifest uniformity [e.g., $\gamma_p=(p-1)$]. At the fully chaotic limit we found $\nu_p=0$, which gives $\gamma_p=p-1$. As was stated before, this corresponds to a uniform distribution.

From most of the hadronic data we infer that $\gamma_p\sim p-1$. This motivates us to look at the previously studied interval between $a=3.9$ and $a=4.0$. For the specific value of $a=3.973052$ the factorial moments are

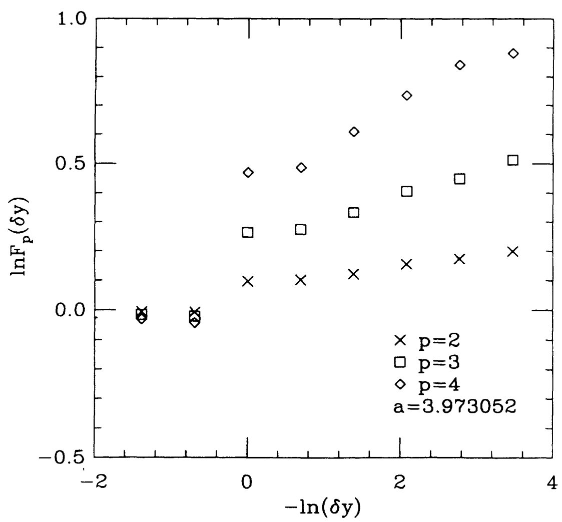

FIG. 11. Factorial moments of the TLM at $a=3.973\,052$.

shown in Fig. 11. The slopes read

$$\nu_2 \simeq 0.0292, \quad \nu_3 \simeq 0.0710, \quad \nu_4 \simeq 0.120 \ , \tag{3.23}$$

with the ratios $\nu_3/\nu_2 \simeq 2.4315$ and $\nu_4/\nu_2 \simeq 4.1095$. The fractal dimensions γ_p are found to be

$$\gamma_2 \simeq 0.9708, \quad \gamma_3 \simeq 1.9290, \quad \gamma_4 \simeq 2.880 \ , \tag{3.24}$$

and the ratios γ_p/γ_{p-1} are

$$\gamma_3/\gamma_2 \simeq 1.987, \quad \gamma_4/\gamma_2 \simeq 2.966 \ . \tag{3.25}$$

The two important things to be considered here are the value of γ_2 and the ratio γ_p/γ_2. The former is the dimension of the pair-correlation function $I_2(\delta y)$. In the strongly intermittent case we have found $\gamma_2 \sim 0$, and in the strongly chaotic limit $\gamma_2 \sim 1$. Hence, the interplay between these limits is an indicator of how uniform the rapidity distribution is. The dynamics of a particular model is, however, reflected in the intermediate region, leaving the strongly intermittent and strongly chaotic limits

TABLE I. ν_p's are adopted from the various experiments and the γ_p's are calculated using Eq. (3.19). Errors in the γ_p's are directly projected from the ν_p's, and for the ratios we use the standard way of taking the larger fractional error to be that of the result.

UA1 [13]	p	ν_p	γ_p	γ_p/γ_2
	2	0.012±0.002	0.988±0.002	1.000
$\sqrt{s}=630$ GeV	3	0.028±0.005	1.972±0.005	1.995±0.005
$p\bar{p}$	4	0.049±0.010	2.951±0.010	2.986±0.010
	5	0.062±0.026	3.938±0.026	3.985±0.026
KLM [20]	p	ν_p	γ_p	γ_p/γ_2
	2	0.027±0.001	0.973±0.001	1.000
200 GeV/nucleon	3	0.080±0.005	1.920±0.005	1.973±0.005
p+Ag/Br	4	0.170±0.019	2.830±0.019	2.908±0.019
	5	0.276±0.046	3.724±0.046	3.827±0.047
NA22 [13]	p	ν_p	γ_p	γ_p/γ_2
	2	0.012±0.001	0.988±0.001	1.000
$\sqrt{s}=250$ GeV	3	0.048±0.002	1.952±0.002	1.975±0.002
π^+p, K^+p	4	0.140±0.010	2.860±0.010	2.894±0.010
	5	0.310±0.020	3.690±0.020	3.734±0.020
TASSO [20]	p	ν_p	γ_p	γ_p/γ_2
	2	0.023±0.003	0.977±0.003	1.000
$\sqrt{s}=35$ GeV	3	0.080±0.014	1.920±0.014	1.965±0.014
e^+e^-	4	0.134±0.052	2.866±0.052	2.933±0.053
KLM [20]	p	ν_p	γ_p	γ_p/γ_2
	2	0.016±0.002	0.984±0.002	1.000
200 GeV/nucleon	3	0.042±0.004	1.958±0.004	1.989±0.004
O+Ag/Br	4	0.080±0.009	2.920±0.009	2.967±0.009
	5	0.131±0.017	3.869±0.017	3.931±0.017
	6	0.195±0.028	4.805±0.028	4.883±0.028

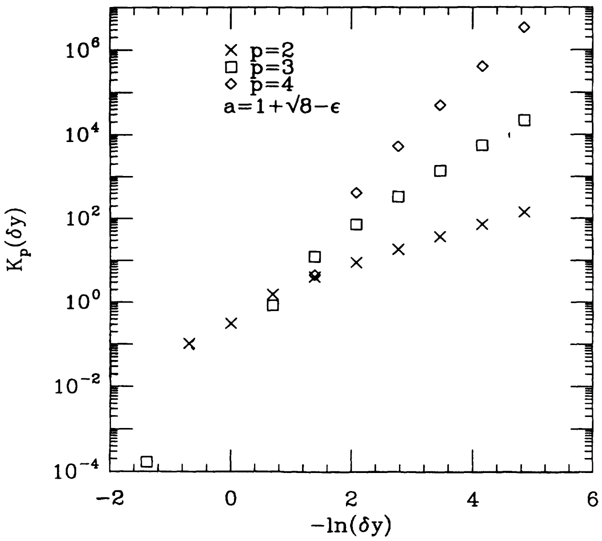

FIG. 12. Factorial cumulants of the intermittent TLM.

to be independent from the particular model being used. The latter, γ_p/γ_2, measures the strength of the phase-space coupling. The achievement of a quantitative fit of the above model to the existing data would be quite surprising. In order to help the qualitative aspects of the methodology above, we present in Table I the fractal dimensions γ_p calculated from the slopes of the hadronic data fits from a few experiments. As a result of the linear relation $\nu_p = p - 1 - \gamma_p$, errors for the ν_p's and γ_p's are the same. We also find that the errors of the ratios γ_p/γ_2 are almost the same as those of the ν_p's. That indicates that by measuring the GP moments and fitting γ_p's one introduces much smaller statistical errors.

2. *Cumulants*

Most of the hadronic data are evaluated by using factorial moments. However, density correlations often contain physically trivial background contributions. In such cases the smooth background has to be removed from the histograms, and in turn the dynamical part of the fluctuations becomes more transparent and reliable. By systematically removing the lower-order density correlations from the higher-order ones, we obtain the cumulants

$$K_p(\delta y) = \frac{1}{M}\sum_{i=1}^{M}\frac{1}{(\delta y)^p}\int_{\Omega_i^{(p)}} dy_1\, dy_2 \cdots dy_p \times \frac{C_p^{(i)}(y_1,\ldots,y_p)}{(\rho_1^{(i)})^p} , \quad (3.26)$$

where the cumulant correlations $C_p(y_1,\ldots,y_p)$ are

$$\begin{aligned} C_2(y_1,y_2) &= \rho_2(y_1,y_2) - \rho_1(y_1)\rho_1(y_2) , \\ C_3(y_1,y_2,y_3) &= \rho_3(y_1,y_2,y_3) - \sum_{i\neq j\neq k}\rho_1(y_i)\rho_2(y_j,y_k) + 2\rho_1(y_1)\rho_1(y_2)\rho_1(y_3) , \\ C_4(y_1,y_2,y_3,y_4) &= \rho_4(y_1,y_2,y_3,y_4) - \sum_{i\neq j\neq k\neq l}\rho_1(y_i)\rho_3(y_j,y_k,y_l) - \sum \rho_2(y_i,y_j)\rho_2(y_k,y_l) \\ &\quad + \sum \rho_2(y_i,y_j)\rho_1(y_k)\rho_1(y_l) - 6\rho_1(y_1)\rho_1(y_2)\rho_1(y_3)\rho_1(y_4) . \end{aligned} \quad (3.27)$$

The set (3.27) and its coefficients, in general, compose a field-theory expression in which $C_p(y_1,\ldots,y_p)$ are the coefficients of the Taylor expansion of the logarithm of the partition functional (generating function) in terms of sources. Thus, a general expression for cumulants is given in terms of derivatives of a generating function [5,21–23]. In the previous subsection we showed that in the absence of correlations the fractal dimensions γ_p become additive in terms of the fractal dimension γ_2 of the two-dimensional rapidity spaces [22]. In the cumulant technique, uncorrelated dimensions do not contribute to the cumulant scaling.

The first few cumulants can be easily written in terms of the F_p's as

$$\begin{aligned} K_2 &= F_2 - 1 , \\ K_3 &= F_3 - 3F_2 + 2 , \\ K_4 &= F_4 - 4F_3 - 3F_2^2 - 6 . \end{aligned} \quad (3.28)$$

We show in Fig. 12 the factorial cumulants corresponding to the intermittent case. The removal of the background effects translates to a large-range scaling of $K_p(\delta y)$'s, including the long-range sector $\delta y \le 1$. An important observation here is that higher cumulants add appreciably to the dynamical description given by the lower ones. If we describe $K_p(\delta y)$ as

$$\ln K_p(\delta y) \sim B_p - \beta_p \ln \delta y , \quad (3.29)$$

we find that $B_p \simeq 1$ and $\beta_2 \simeq 0.9984$, $\beta_3 \simeq 2.0635$, $\beta_4 \simeq 3.2501$.

Results are shown for $K_p(\delta y)$ at $a=3.9$ and $a=3.973\,052$ in Fig. 13. The dynamics in this regime is dominated by two-particle cumulants indicated by the small contributions of higher cumulants as compared to K_2. For a pure chaotic (Gaussian) distribution cumulants of $p>2$ vanish, and for a pure Poissonian distribution factorial cumulants of $p \ge 2$ vanish. Neglecting the difference in the data between factorial and ordinary cumulants [which is $O(1/\langle n\rangle)$], we infer that our model is closer to Gaussian distribution in the chaotic limit. Recently such vanishing hierarchy of cumulants has been observed [24] in the UA1 data. According to observa-

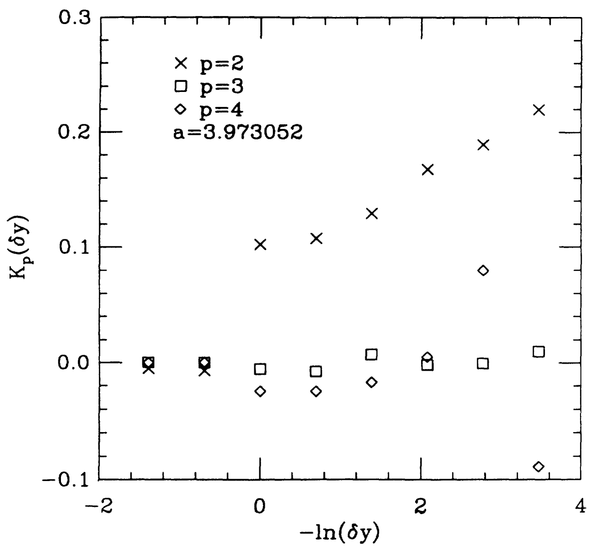

FIG. 13. Factorial cumulants of the TLM at $a = 3.973\,052$.

tion, the factorial moments F_p acquire 70–90% of their value solely from the second cumulant K_2, and the relative contribution of K_2 as compared to $K_p(p>2)$ increases as $\delta y \to 0$. Although it is dominated by two-particle correlations, the dynamics of hadron production is not completely chaotic. Remarkably, for UA1 (also with UA5 and NA22 this includes both nuclear and hadronic targets) $K_3(\delta y)$ is small but nonvanishing such that the linked-pair coefficient $K_3/(K_2)^2$ is almost bin-size independent and close to the value given by the negative binomial distribution. For the manifestly Gaussian fluctuation linked-pair coefficients would vanish, whereas for a strongly nonuniform fluctuation the linked-pair approximation would not work at all. This is the limit described by weak intermittency at one end and short-range correlations at the other.

IV. CONCLUSIONS

In this work a qualitative understanding of hadronic intermittency has been attempted by deductive use of simple finite fractal sets. Arguments of general validity such as the relative magnitude of the slopes of the factorial moments generated by strongly intermittent or smooth distributions and conditions for translation invariance and its effects on the fractal dimensions are shown to enhance understanding of the hadronic phase-space correlations. Such general features have no model dependence at the limits of full and no correlations, enabling the use of generic models. Perhaps this explains why there are so many ideas that can be fitted equally well to the experimental data.

Translation invariance is frequently assumed in hadronic correlations. In Sec. II we showed that "fake" violations of TI can be cured controllably by smoothly transforming the rapidity distribution. It was also shown that this process does not change the behavior of the dynamical system, hence leaving the moments and other correlations intact. Actually this is the idea behind the vertical moments recently introduced in order to suppress the spikes and enhance the valleys of the rapidity distribution [24]. This process is the numerical analogue of the transformations introduced in Secs. II and III. In the cases for which one cannot recover TI by defining smooth transformations in the rapidity, the assumption of translation invariance leads to the undesirable consequence of obscuring the genuine dynamical structures. It is pointed out in Ref. [25] that in such non-TI cases, statistical theorems derived for manifest TI are not valid. A particular case is the Wiener-Khinchin ergodic theorem [26], which relates the power spectrum of the one-particle rapidity distribution to the Fourier transform of the two-particle correlation function. This theorem is violated by the fact that the duality between the rapidity and its conjugate variable, i.e., the eigenvalue of the longitudinal boost operator [27], is lost; specifically, the two are not uniquely linked by a Fourier transform. This motivates an independent phenomenological analysis of the phase space in terms of both the rapidity and the boost. In this respect we also consider the boost variable as an essential component of the intermittency analysis.

There is a close connection between scaling indices of the moments and the fractal dimensions of the multifold phase space. The magnitude and the ratios of these fractal dimensions project the dynamical structure of the phase space, resolving the degree of nonuniformity. By applying this to the hadronic data fits of the slopes we found that the dynamical structure of the phase space is close to the one expected from a uniform chaotic distribution. The relative statistical error introduced by fitting the fractal dimensions, rather than the factorial moment slopes, is much smaller, giving merit to using the phase-space analysis and to the GP moments.

Note added. After this work was completed, the author became aware of Ref. [28], where hadronic intermittency is contrasted with the intermittency in the mathematical context. This correspondence is also the central point in this work.

ACKNOWLEDGMENTS

The author is indebted to P. Carruthers for his encouragement and support. He also acknowledges the hospitality of the Aspen Physics Institute. This work was supported by the U.S. Department of Energy, Divisions of High Energy and Nuclear Physics.

[1] UA1 Collaboration, G. Arnison *et al.*, Phys. Lett. B **226**, 410 (1989); UA5 Collaboration, G. J. Alner *et al.*, Phys. Lett. **160B**, 193 (1985); ABCDHW Collaboration, A. Breakstone *et al.*, *ibid.* **114B**, 383 (1982).
[2] G. Goldhaber, S. Goldhaber, W. Lee, and G. Pais, Phys. Rev. **120**, 840 (1962).
[3] R. Hanbury Brown and R. Q. Twiss, Proc. R. Soc. London **A242**, 300 (1957); **A243**, 291 (1957).

[4] G. Goldhaber *et al.*, Phys. Rev. **120**, 300 (1960).
[5] P. Carruthers and C. C. Shih, Int. J. Mod. Phys. A **2**, 1447 (1987).
[6] A. Bialas and R. Peschanski, Nucl. Phys. **B273**, 703 (1986); **B308**, 857 (1988).
[7] P. Carruthers, Phys. Rev. A **43**, 2632 (1991).
[8] P. Carruthers and I. Sarcevic, Phys. Rev. Lett. **63**, 1562 (1989).
[9] P. Carruthers, H. C. Eggers, and I. Sarcevic, Int. J. Mod. Phys. A **6**, 3031 (1991).
[10] P. Grassberger and I. Proccacia, Phys. Rev. Lett. **50**, 346 (1983); Physica D **9**, 189 (1983); I. M. Dremin, Mod. Phys. Lett. A **3**, 1333 (1988).
[11] P. Carruthers, Int. J. Mod. Phys. A **4**, 5587 (1989).
[12] T. Hakioḡlu, Ph.D. thesis, University of Arizona, 1991.
[13] UA1 Collaboration, C. Albajar *et al.*, Nucl. Phys. **B345**, 1 (1990); UA5 Collaboration, R. E. Ansorge *et al.*, Z. Phys. C **43**, 357 (1989); NA22 Collaboration, I. V. Ajinenko *et al.*, Phys. Lett. B **235**, 373 (1990).
[14] P. Lipa and B. Bushbeck, Phys. Lett. B **223**, 465 (1989).
[15] T. Hakioḡlu, in *Intermittency in High Energy Collisions,* Proceedings of the Workshop, Santa Fe, New Mexico, 1990, edited by F. Cooper, R. Hwa, and I. Sarcevic (World Scientific, Singapore, 1991).
[16] Ya. B. Zeldovic, S. A. Molchanov, A. A. Ruzmaikin, and D. D. Sokolov, Usp. Fiz. Nauk **152**, 3 (1987) [Sov. Phys. Usp. **30**, 353 (1987)].
[17] P. Berge, M. Dubois, P. Manneville, and Y. Pomeu, in *Universality in Chaos,* edited by P. Cvitanovic [J. Phys. Lett. (Paris) **41**, 341 (1980)].
[18] Y. Pomeau and P. Manneville, Commun. Math. Phys. **74**, 189 (1980).
[19] J. E. Hirsh, B. A. Huberman, and D. J. Scalapino, Phys. Rev. A **25**, 519 (1982).
[20] KLM Collaboration, R. Holynski *et al.*, Phys. Rev. C **40**, 2449 (1989); TASSO Collaboration, W. Braunschweig *et al.*, Phys. Lett. B **231**, 549 (1989).
[21] M. Kendall and A. Stuart, *The Advanced Theory of Statistics* (Griffin, London, 1977).
[22] C. D. Cantrell, Phys. Rev. A **1**, 672 (1970).
[23] R. F. Chang, V. Korenman, C. O. Alley, and R. W. Detenbeck, Phys. Rev. **178**, 612 (1969); R. Kubo, J. Phys. Soc. Jpn. **17**, 1100 (1962).
[24] P. Carruthers, H. C. Eggers, and I. Sarcevic, Phys. Lett. B **254**, 258 (1991).
[25] P. Carruthers and T. Hakioḡlu, Phys. Rev. D (to be published).
[26] W. Goodman, *Statistical Optics* (Wiley, New York, 1986).
[27] B. Durand and L. O'Raifeartaigh, Phys. Rev. D **13**, 99 (1976).
[28] J. Dias de Deus, Phys. Lett. B **194**, 297 (1987).